Doctoral School of the Faculty of Applied Sciences

Session Program
PHYSICS

BN 134 - 25.05.2017

OPENING SESSION	9:00-9:20

Welcome address	*Prof. Niculae PUŞCAŞ, Director of Doctoral School*
Opening address	*Eng. Drd. Bogdan Ştefăniţă CĂLIN, Member of Doctoral School Board*

SESSION ONE	9:20-11:20

Chair, *Andreea Mitu, Doctoral School of the Faculty of Applied Sciences*

1. Implementing refraction correction for laser beam diagnostics and alignment at CETAL petawatt-class laser
Mihail-Gabriel Bărbuţă

2. Polarization beam splitter design based on slab photonic crystals for two-photon polymerization direct laser writing
Bogdan Ştefăniţă Călin, Marian Zamfirescu, Radu Ionicioiu, Niculae Puscas

3. Investigation of dissimilar laser welding of stainless steel to aluminium in lap joints configuration
G.D. Chioibaşu, D. Klobčar, D. Sporea, S. Smolej and A. Nagode

4. NO_2 total column amount from Pandora – 2S, comparison with satellite data: Preliminary results
Alexandru Dandocsi, Anca Nemuc, Niculae Puscas, Liliana Preda

5. Laser matter interaction
Ioana Dinicu (Spirea)

6. A conservative or dissipative Universe? Gravitational viscosi and the space---time torsion. From COBE to Gravity Probe
Cristian Gheorghiu

PAUSE	11:20-11:40

SESSION TWO	11:40-13:20

Chair, *Mihail-Gabriel Bărbuţă, Doctoral School of the Faculty of Applied Sciences*

7. Thin film deposition using the pulsed laser method
Oana Andreea Lazăr

8. High grade decontamination of Ni targets for sub-barrier transfer reactions
Andreea Mitu, Marius Dumitru, Florian Dumitrache, Nicolae Marginean, Rareş Şuvailă, Cristina Niţă, Maria Dinescu, Gheorghe Căta -Danil

9. **The study of p-Si/TiO$_2$/n-Si (100) sandwiches structures deposited by KrF excimer laser ablation**
Călin Moise, Alin Jderu, Oana Brincoveanu, Dionizie Bojin, Marius Enăchescu

10. New digital acquisition system for alarge multichannel spectroscopy array
Lucian Stan

11. Assessment of a Hybrid Acquisition System for Positron Annihilation-based Spectroscopy
Sebastian Toma

CLOSING SESSION	13:20-13:40

Chair, *Bogdan Ştefăniţă CĂLIN, Doctoral School of the Faculty of Applied Sciences*

Implementing refraction correction for laser beam diagnostics and alignment at CETAL petawatt-class laser

Mihail-Gabriel Bărbuță

Faculty of Applied Sciences, "Politehnica" University, Bucharest

Abstract

Complex high-power laser installations which require multiple mirrors in high vacuum conditions also require multiple diagnostics points to ensure that the laser beam is properly aligned before starting experiments. In some cases, the diagnostics beam is acquired using transmitted (leaked) beam from the rear of the alignment mirrors, but the refractive index of these mirrors will induce a deviation of the diagnostics beam position, which itself varies according to the mirror relative inclination. Correcting this deviation needs to be implemented in automated and manual beam alignment systems, to avoid clipping and internal reflections which can be detrimental to laser system infrastructure.
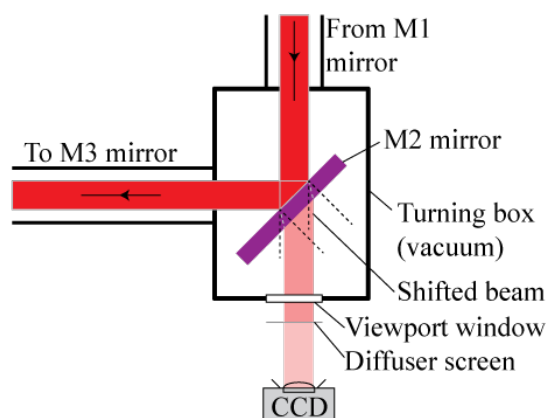
Fig. 1 – Conceptual representation of laser diagnostics beam displacement

For implementing refraction correction into beam alignment algorithms, a optical study has been conducted at INFLPR CETAL petawatt laser system, taking several factors into consideration: laser parameters, beam transport system design, mirror constructive details and material parameters. Beam deviation tests have been conducted at various mirror inclinations and results were compared with calculated deviation interval.
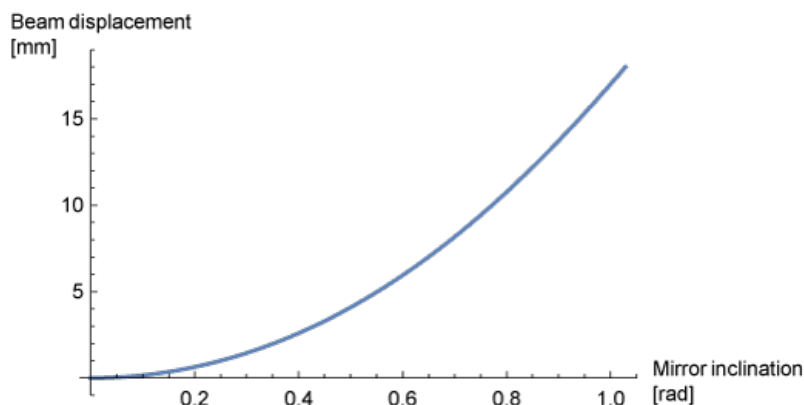

Fig. 2 – Calculated beam displacement variation function of mirror inclination
(sapphire, 65 mm thickness, P-polarized laser beam)

The existing alignment algorithms for CETAL's beam transport system were updated to include mirror-angle-driven refraction correction. Encoded mirror inclination values are captured, and corresponding refraction deviation is automatically calculated by an additional algorithm written in Python programming language. The alignment software then calculates the correct beam centroid. This implementation resulted in significant improvement in alignment and beam centering accuracy, correcting centering calculations for diagnostics beam shifts up to 18 mm in extreme mirror tilt situations.
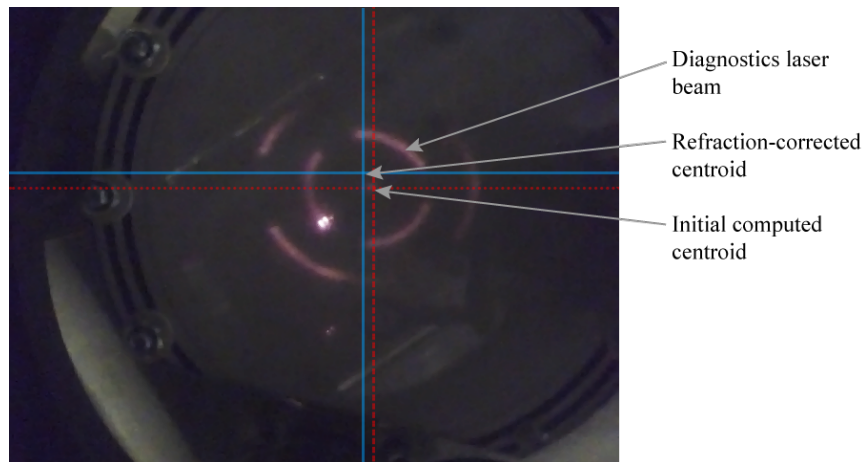

Fig 3 – Laser beam centering diagnostics with initial and corrected centroid calculation

Scientific literature search has revealed no previous studies of refraction correction for laser beam diagnostics and alignment. This solution can be implemented in existing and future high-power laser systems to aid in achieving higher alignment precision and efficiency, and can be easily adapted to various material and laser parameters.

List of references:
1. Wolf, K. B., "Geometry and dynamics in refracting systems", European Journal of Physics 16: 14-20, 1995
2. ARDoP SAS, "CETAL Project – Beam Line Transportation – Final design", 2013
3. Harman, Alang Kasim; Ninomiya, Susumu; Adachi, Sadao, "Optical constants of sapphire (alpha-Al2O3) single crystals". Journal of Applied Physics. 76 (12): 8032–8036 (1994)

POLARIZATION BEAM SPLITTER DESIGN BASED ON SLAB PHOTONIC CRYSTALS FOR TWO-PHOTON POLYMERIZATION DIRECT LASER WRITING

B. Calin[1], M. Zamfirescu[1], R. Ionicioiu[2], N. Puscas[3]

Integrated polarization beam splitters and photonic crystals represent complex optical microstructures with various applications. Photonic crystals may be used in fiber fabrication for more efficient light confinement [1] or as wavelength filters [2], due to the existence of photonic band gaps. Furthermore, these band gaps can manifest for specific polarizations of incident light, which not only extends the applications of photonic crystals as filters, but they can also be employed in complex optical structures that act as polarization beam splitters [3], [4], [5].

In this paper, a complex photonic structure acting as a narrow-band polarization beam splitter is discussed. Apart from a two-dimensional photonic crystal with a TE band gap centered around a wavelength of 780 nm, the device is comprised of linear waveguides, parabolic light "collectors" (parabolic tapered waveguides) and multimode interference couplers. A schematic of the device is presented in figure 1.

A step-by-step methodology for the optimization of the photonic crystal is presented. Device fabrication is also addressed as the targeted method is based on two-photon polymerization direct laser writing. Experimental results are discussed and compared to other largely utilized methods such as simple direct laser writing [6], lithography [7], autocloning [8] and others [2].
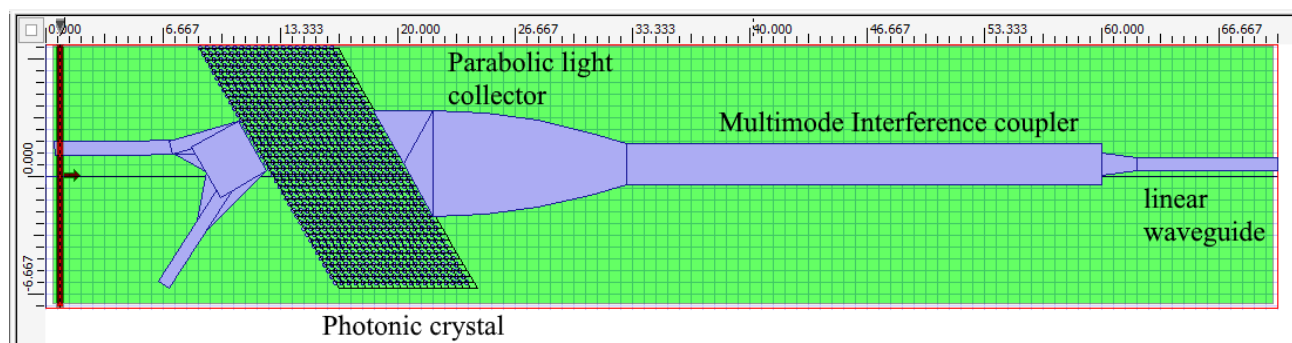

Figure 1: Polarization beam splitter design.

R E F E R E N C E S

[1] *J. Kim, H. K. Kim et. al.,* The Fabrication of a Photonic Crystal Fiber and Measurement of its Propoerties, Journal of the Optical Society of Korea, **vol. 7**, no. 2, pp. 79-83, (2003);

[2] *Y. Ohtera et. al.,* Ge/SiO2 Photonic Crystal Multichannel Wavelength Filters for Short Wave Infrared Wavelengths, Japanese Journal of Applied Physics, **vol. 46**, no. 4A, pp. 1511-1515, (2007);

[3] *E. Schonbrun et. al.,* Polarizaiotn beam splitter based on a photonic crystal heterostructure, Optics Letters, **vol. 31**, no. 21, pp. 3104-3106, (2006);

[4] *J. She et. al.,* High-efficiency polarization beam splitters based on a two-dimensional polymer photonic crystal, Journal of Optics A: Pure and Applied Optics, **vol. 8**, pp. 345-349, (2006);

[5] *W. Zheng et. al.,* Integration of a photonic crystal polarization beam splitter and waveguide bend, Optics Express, **vol. 17**, no. 10, pp. 8657-8668, (2009);

[6] *J. Haberko et. al.,* Fabrication of mesoscale polymeric templates for three-dimensional disordered photonic materials, Optics Express, **vol. 21**, no. 1, pp. 1057-1065, (2013);

[7] *M. Belotti et. al.,* All-optical switching in 2D silicon photonic crystals with low loss waveguides and optical cavities, Optics Express, **vol. 16**, no. 15, pp. 11624-11636, (2008);

[8] *C. C. Cheng et. al.,* New fabrication techniques for high quality photonic crystals, Journal of Vacuum Science and Technology B, **vol. 15**, no. 6, pp. 2764-2767, (1997);

Investigation of dissimilar laser welding of stainless steel to aluminium in lap joints configuration

G.D. Chioibaşu[1], D. Klobčar[2], D. Sporea[1], S. Smolej[3] and A. Nagode[3]

1. National Institute for Laser Plasma and Radiation Physics, 077125 Magurele, Romania
2. University of Ljubljana, Faculty of Mechanical Engineering, Aškerčeva 6, 1000 Ljubljana, Slovenia
3. University of Ljubljana, Faculty of Natural Sciences and Engineering, Aškerčeva 12, 1000 Ljubljana, Slovenia

Due to the many advantages given by dissimilar materials welded joints, like weight saving, reduction of pollutant emissions, the application of different welding components made of steel and aluminium alloys is still researchable. Laser fiber welding in a lap joint configuration of low carbon stainless steel, SS 316 L and A1050 aluminium alloy with 1 mm thick is presented. Tests that have undergone procedures are: tensile tests, optical metallography and scanning electron microscopy. A fibre laser with 400 W power in CW mode was used and the process parameters like speed and focusing position were optimized.

Keywords: Dissimilar SS - Al welding; Fiber Laser welding; Lap joint configuration; Tensile strength.

1. Introduction

Welding dissimilar materials technology is continuously growing, but is a big challenge in engineering, because of the many advantages that this process offers to industry. Such as, good mechanical properties and corrosion resistance [1]. Joining stainless steel and aluminium reduce the weight of the car body and the consumption of fuel [2]. In laser welding the process parameters, like laser power, welding speed and focused position are essential. The optimized values of this factors can be obtain by using numerical optimization [3].

2. Experimental procedures

In the present study, the materials used were a low carbon stainless steel, SS 316 L and A1050 aluminium alloy with 120 mm x 40 mm x 1 mm. The chemical composition and mechanical properties are presented in the Table 1 and 2, respectively. Both materials were cleaned with alcohol and dried at warm air before welding, in order to get best quality of welds.

Table 1 Chemical composition of AISI 316L and A 1050(weight %).

Material	Elements (wt %)									
	C	Si	Mn	P	S	Cr	Mo	Ni	N	Fe
AISI 316 L	≤0.03	≤0.7	≤2	≤0.04	≤0.03	18	2-3	10-14	≤0.1	Balance

Material	Elements (wt %)							
	Cu	Mg	Si	Fe	Mn	Zn	Ti	Al
A 1050	≤0.05	≤0.05	≤0.25	≤0.4	≤0.05	≤0.07	≤0.05	Balance

A fiber laser was used for welding experiments, with a maximum power of 400 W in continuous mode (IPG Photonics, model YLR-400-AC, wavelength1070 nm). A three-dimensional scanning head (HighYAG, RLSK) was attached to a six axis robot machinery (Motoman MC2000). During the welding process a cooper backing plate was under the working pieces to absorb a part of the head due to the laser processing.
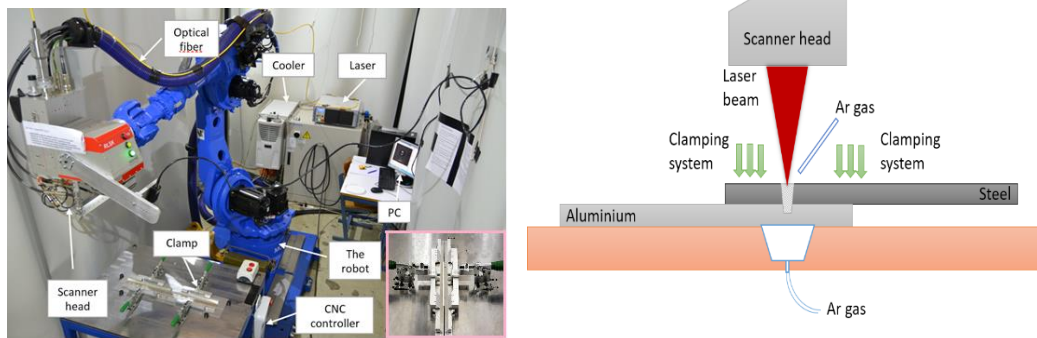
Fig. 1. Set-up experiment

3. Results and analysis

Five sets of optimized welding parameters process were performed in order to confirm the valability of the optimal results. SEM analysis (fig. 2) and macro-section of optimized weld were carried out to verify the quality of the welds.
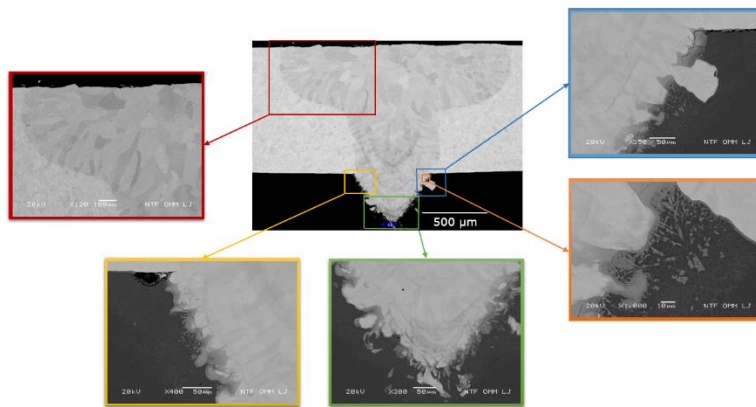
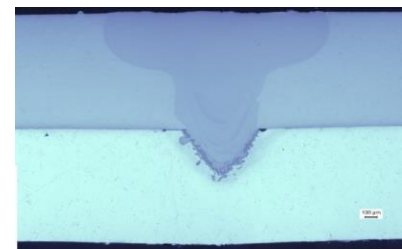

Fig. 2 SEM analysis of optimized weld

Fig. 3 Macro-section of optimized weld

4. Conclusions

✓ The best value of tensile strength it was achieved when a small part of stainless steel was meld into aluminium

✓ As deeper the weld is so many crack and defects appear

✓ The best weld was obtained by using 1.5 m/min speed and 0.5 mm defocus

References

1. Chen, S., Huang, J., Xia, J., Zhao, X., & Lin, S. *Influence of processing parameters on the characteristics of stainless steel / copper laser welding*, Journal of Materials Processing Technology. *222*, 43–51, (2015).
2. Sierra G, Wattrisse B, Bordreuil C. *Structural analysis of steel to aluminium welded overlap joint by digital image correlation*. Exp Mech (2008).
3. A. Ruggiero , L.Tricarico , A.G.Olabi , K.Y.Benyounis, *Weld-bead profile and costs optimisation of the CO2 dissimilar laser welding process of low carbon steel and austenitic steel AISI 316,* Optics & Laser Technology, 43 ,82–90 (2011)

NO_2 total column amount from Pandora – 2S, comparison with satellite data: Preliminary results

A. Dandocsi[1,2], A. Nemuc[1], N. Puscas[2], L. Preda[2]
[1]National Institute of R&D for Optoelectronics, Magurele, Romania, *e-mail:
alexandru.dandocsi@inoe.ro
[2]University Politehnica of Bucharest, Romania

Introduction

The NO_2 in an important atmospheric pollutant that can be toxic in certain concentrations and the chemical reaction within the atmosphere ($NO_x = NO + NO_2$) leads to the production of ozone and aerosols. It is mainly produced by the anthropogenic activities like industry, traffic, forest fires but it can be produced in the natural way also [1].

The NO_2 total column amount is monitored from the satellite instruments since 1995, last system launched with this purpose being Ozone Monitoring Instrument (OMI), launched in 2004. Ground based measurements from a Pandora – 2S system, part of the Pandonia network (www.pandonia.net) are used in comparison with OMI retrieval in order to participate in the calibration / validation activities of the satellite. Other similar studies have been made by [2]

Instruments description

The Pandora – 2S system is a Multi Axis Differential Optical Absorption Spectroscopy system capable of having direct Sun/Moon measurements or measurements at different zenith and azimuth angles. The system has two spectrometers, ranging from 290 nm to 900 nm with a 0.6 nm resolution for the first spectrometer and a 1.1 nm resolution for the second spectrometer.The system uses direct Sun/Moon measurements in order to retrieve the total column amount of NO_2 and O_3. The AirMassFactor (AMF), factor needed for the total column amount calculation, is obtained using the secant of the Solar Zenith Angle (SZA). For SZA greater than 80^0, spherical atmosphere corrections must be applied [2].Global measurements of NO_2 are made using the Ozone Monitoring Instrument placed on board of the Dutch-Finnish satellite of NASA, Aura EOS (Earth Observation System). The measurements are provided almost daily with a nominal spatial resolution of 13 x 24 km^2 at nadir since October 2004[3]. The NO_2, among other trace retrieval is made using the solar backscatter light in the UV-VIS spectral range, measured by a two-dimensional CCD (charge-coupled device) detector.

The total column amounts of NO_2 from both systems were retrieved using the fixed location of the Pandora system which is near Bucharest, at approximately 12 kilometers from the city center, in the southern region. The pre-urban area, where the Pandora is located, is influenced from the highly active ring road traffic but also from the rural area,agricultural activities. In other words, the location is equally influenced by both natural and anthropogenic emissions.

Methodology

Retrieval of total column amount of NO_2 is based on direct sun measurements and it can be done using both spectrometers, using the absorption cross section from [4]. The satellite data are retrieved using the solar backscattered light in the UV-VIS region but the NO_2 total column amount is calculated using the similar processing as for the ground based measurements.

For this paper, the level 2 global gridded data were used with a 0.25 deg. x 0.25 deg. resolution. Each data point selected for this study was carefully investigated. The location was selected within a ± 0.4 deg. from the ground based system. After that, the cloud cover parameter was taken into consideration so the data should not be influenced by the high reflectivity of the clouds.

From the ground based measurements point of view, data were selected around the time of the satellite overpass with a ± 1 hour bias, and then the mean value and its error were computed. Another way of using satellite data is to take only the automatically generated measurements for different locations(gome). This data file contains only the latitude and longitude of the measurement and the total column amount of interested absorber.The spectral range from which the total column of NO_2 is computed is between 400 nm and 440 nm for the Pandora system and 405 nm and 465 nm for the satellite data.

Results and discussions

Two months of ground based measurements of total column amount of NO_2 was selected for this study.For comparison Starting from the satellite data described in the methodology section and then selecting the Pandora measurements, the total column amount of NO_2 was computed.
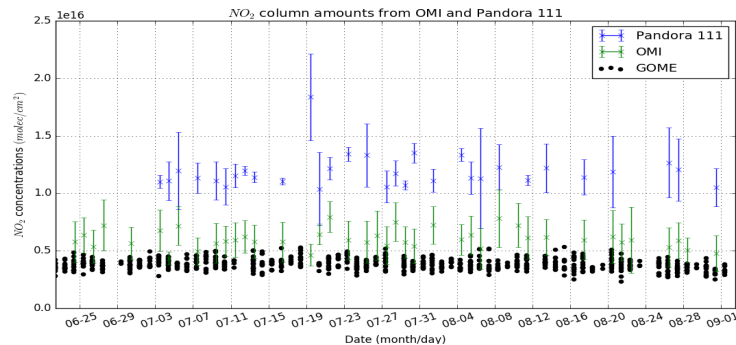

Figure 1 Total column amount of NO_2 from Pandora measurements and OMI satellite, July – August 2016

Figure 1 shows retrievals from ground based and satellite instruments where the black marker was used for the automatically generated data from satellite measurements around a fixed location. The difference between the two systems could be explained by different calibration proceduresof each of the instruments. The Pandora system it is calibrated using a 9 step process using clear sky measurements as described by [2]. Data selected from the level 2 gridded measurements show similar trend to the ones from Pandora as they tend to have similar variation from day to day while the automatically generated data tend to be more stable (Not Shown).

Conclusions

Total column amount of NO_2 from a ground based instruments was retrieved in order to be compared with coincident satellite measurements and a period of two months is presented here.One algorithm of data selection from satellite measurements is presented in order to compare the total column amounts of NO_2 with the ground based measurements. A bias in the absolute values from the two instruments, further analysis will be done.

References

[1] Wenig, M. O., et.al. (2008), Validation of OMI tropospheric NO2 column densities using direct-Sun mode Brewer measurements at NASA Goddard Space Flight Center, J. Geophys. Res., 113, D16S45, doi:10.1029/2007JD008988

[2] J. Herman, et.al., *NO₂ column amounts from ground-based Pandora and MFDOAS spectrometers using direct-sun DOAS technique: Intercomparison and application to OMI validation,* Journal of Geophysical Research, Vol. 114, D13307, doi:10.1029/2009JD011848, 2009

[3]Levelt, P. F, et. al.: *The Ozone Monitoring Instrument,* IEEE T. Geosci. Remote, 44, 1093–1101, doi:10.1109/TGRS.2006.872333, 2006.

[4] Vandaele, A.C., et.al.,*Measurements of the NO2 absorption cross-section from 42 000 cm–1 to 10 000 cm–1 (238-1000 nm) at 220 K and 294 K, J. Quant. Spectrosc. Radiat. Transfer, 59 (3-5), 171-184, 1998

LASER MATTER INTERACTION

AUTHOR:Dinicu (Spirea) Ioana

GUIDING TEACHER: Prof. Univ. Dr. Niculae PUŞCAŞ

Summary

In this paper ,the fundamental theoretical and numerical approaches developed to analyse laser–target interaction, plasma formation, as well as its expansion will also be reviewed, and their predictions compared with the experimental findings. Although the main emphasis of the review will be on metal target ablation, reference and comparison to results on multicomponent targets will also be frequently given.
The generation of high-density and high-temperature plasmas by focusing high peak power laser radiation onto a solid target is still a growing field in basic science, engineering and material processing technology (Von Allmen and Blatter 1995, Miller and Haglund 1998),though the interaction of laser light with materials and the properties of the plasma produced have been investigated for many years (Kennedy 1984). The strong interest in this field is largely due to the fact that both fundamental aspects of laser–solid interaction and consequent plasma generation, and applied techniques in material processing technology and sample elemental analysis are involved (Bauerle 1984, 1996).

Since laser ablation depends on the target thermo-physical properties and laser beam parameters. The scope of the paper is to study,especially,the ablation process of simple one-component materials suchas metals **(ex. Al, Cu, Fe)** which allow a better comprehension of the basic mechanisms involved in laser–solid and laser–plasma interaction. Since the thermo-physical properties of metals are comparatively well known, they will be compared to experimental data.

Is taken into account the *adiabatic limiting case* description of the process: the decoupling of these processes (heating and expansion of the ablated material).
The interaction of high-intensity laser pulses with a solid target involves laser–solid interaction and plasma formation. The process can be divided into two different regimes:
1. at low laser fluence the vapour produced by the leading edge of the laser pulse behaves like a thin medium and the laser beam passes nearly unattenuated through the vapour.
2. at high laser fluence the vapour temperature is high enough to cause appreciable atomic excitation and ionization. Then the vapour begins to absorb the incident laser radiation leading to vapour breakdown and plasma formation.
Laser systems with pulse durations variable from about 100 fs to several nanoseconds allow to perform a very detailed analysis of the laser–matter interaction at different laser pulse durations, leaving the other laser parameters almost unchanged.
In order to understand the basic characteristics of the laser–solid interaction, simple approximated calculations based on energy balance considerations can be applied. This allows an estimation of the order of magnitude of the laser fluence threshold for vaporization, the amount of material evaporated per pulse, as well as its dependence on the laser fluence.
Both the basic physics of the laser–solid interaction and the experimental results show that short laser pulses (610 ps FWHM) offer the advantage of removing material from the target surface without a significant transfer of energy to the surrounding areas, what is of interest in the field of micro-machining and in material processing applications.

Table 1:
Theoretical and experimental fluence threshold, penetration length (short pulse) and absorbance (long pulse) for copper laser ablation at 248 nm. The discrepancy between theabsorbance standard-reference book value and the experimental one can be ascribed to the target shielding due to the vapour formed above the target surface.

Pulse duration = 0.5 ps		Pulse duration = 20 ns	
F_{th} (J cm^{-2}) calculated	0.10	F_{th} (J cm^{-2}) calculated	1.2
F_{th} (J cm^{-2}) fit to equation (5)	0.17	F_{th} (J cm^{-2}) fit to equation (5)	1.5
α^{-1} (nm) literature	14	A literature	0.6
α^{-1} (nm) fit to equation (5)	14.3	A fit to equation (7)	0.03

Figure 1. Ablation depth per pulse versus fluence for 248 nm KrF laser ablation of copper in vacuum: ◯, short pulse (0.5 ps) (after Preuss *et al* 1995); ●, long pulse (20 ns) (after Lunney1995). The full curves are fits according to equations (4) and (6), respectively.
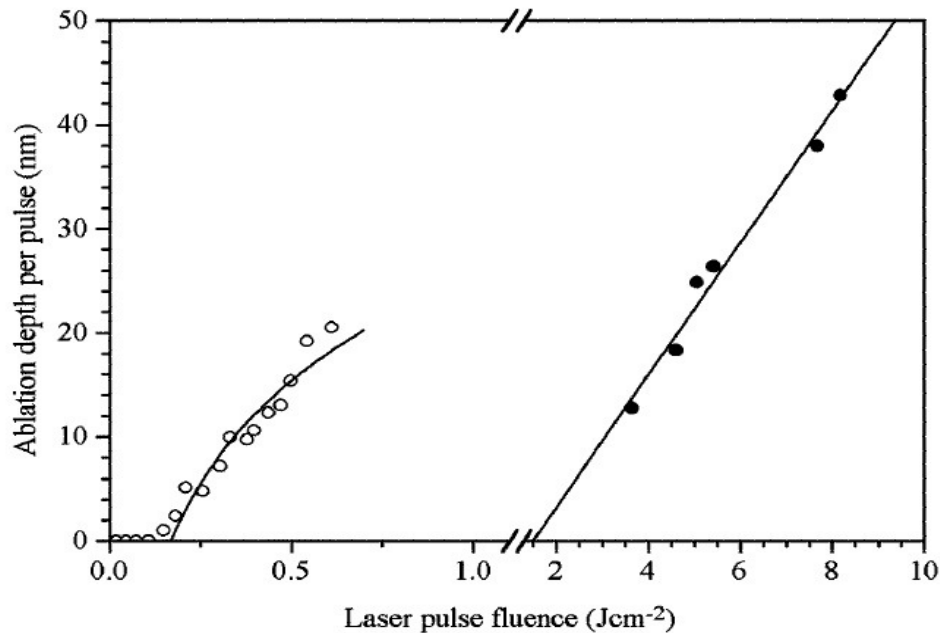
References

Amoruso S 1998 *PhD Thesis* Universit`a degli Studi di Napoli 'Federico II', Naples
——1999 *Appl. Surf. Sci.* **138–139** 292
Amoruso S, Armenante M, Berardi V, Bruzzese R and Spinelli N 1997 *Appl. Phys.* A **65** 265
Amoruso S, Berardi V, Bruzzese R, Spinelli N and Wang X 1998 *Appl. Surf. Sci.* **127–129** 953
Amoruso S, Berardi V, Bruzzese R, Velotta R and Armenante M 1996 *Appl. Phys.* A **62** 533
Amoruso S, Bruzzese R, Velotta R, Spinelli N and Wang X 1999 *Appl. Surf. Sci.* **138–139** 250
Afonso C N, Serna R, Catalina F and Bermejo D 1990 *Appl. Surf. Sci.* **46** 249
Alimpiev S S, Belov M E, Mlinsky V V, Nikiforov S M and Romanjuk V I 1994 *Appl. Phys.* A **58** 67
Bauerle D (ed) 1984 *Laser Processing and Diagnostics* (Berlin: Springer)
——1996 *Laser Processing and Chemistry* (Berlin: Springer)
Bekefi G, Deutsch C and Yaakobi B 1976 *Principles of Laser Plasmas* ed G Bekefi (New York: Wiley) pp 549–641
Berardi V, Amoruso S, Spinelli N, Velotta R, Allegrini M and Arimondo E 1994 *J. Appl. Phys.* **76** 8077
Berardi V, Amoruso S, Spinelli N, Velotta R, Fuso F and Arimondo E 1995 *Int. J. Mass Spectrom. Ion Phys.* **144** 1
Berardi V, Spinelli N, Velotta R, Armenante A, Fuso F, Allegrini M and Arimondo E 1993 *Phys. Lett.* A **179** 116
Boardman A D, Cresswell B and Anderson J 1996 *Appl. Surf. Sci.* **96–98** 55
Callies G, Schittenhelm H, Berger P and Hugel H 1998 *Appl. Surf. Sci.* **127–129** 134
Carslow H S and Jaeger J C 1959 *Conduction of Heat in Solids* (Oxford: Oxford University Press)
Caruso A and Gratton R 1968 *Plasma Phys.* **10** 867

Presentation of work: oral presentation (Microsoft Power Point)
Date: 5 April 2017

A conservative or dissipative Universe? Gravitational viscosity and the space-time torsion. From COBE to Gravity Probe

Cristian Gheorghiu^1

The aim of this paper is to answer the question: "Why are most phenomena in the Universe irreversible" when the theoretical physics is based mainly on conservative principles: energy, impulse or angular momentum!? We know from the 2nd principle of thermodynamics that the general entropy of the Universe only increases and the Universe is deeply dissipative. Paradoxically, physics is generally oriented on the study of the so called " body- forces " : gravitation, electromagnetism, inertial forces, etc. which are conservative fields . But opposed to the body-forces are the so called contact-forces (meaning friction forces, normal forces or viscous forces) which are dissipative and consequently are responsible for the irreversibility of the phenomena of the Universe. In this paper we analyze the primary source of the existence of these dissipative contact forces , namely the space-time's viscosity (i.e. gravitational viscosity [1]). Andrei Linde said that "...scalar field equations that describe the Quantum Vacuum are susceptible to the term of a viscosity ..." [2] . Therefore, we assume the Universal space-time itself as being a viscous fluid and not a perfect one as considered in the General Theory of Relativity (GRT). The main argument for such a hypothesis is the anisotropy measured by COBE in the CMB (Cosmic Microwave Background) in 1993 [3] . In order to test the validity of the value obtained in the paper for the space-time viscosity, we calculate within the paper the space-time's torsion around the Earth (already anticipated by the GRT and confirmed experimentally by the Gravity Probe in 2004): hence the novelty of this study is given by the interpretation of the space-time as a viscous fluid, and the gravitational torsion as a vortex appearing as a Oseen type solution for the Navier-Stokes equation applied to the movement of the Earth through it..

The main result of this article is the determination of the viscosity of the space-time η_0 (named - gravitational viscosity) using 2 different methods (chapter **2**) respectively the method of autocorrelation functions from the Kubo-Green formula, applied to the anisotropies measured by COBE (fig **1**) but also the method of the kinetic-molecular theory for gases. In chapter **4** we have used the value for the gravitational viscosity to calculate the space-time torsion (fig **2**) in conditions similar to the experiment Gravity Probe B and the value obtained here is similar to the frame dragging-drift rate(anticipated by Einstein in GRT) and measured by the Gravity Probe B. This result encourages the use of the viscous fluid model for the space-time in other astrophysics theories. In chapter **5** we have determined, using the Stokes method, the energy lost by the Earth by viscous friction with the space-time in its relative movement through the CMB with the speed of 390 km/s (also determined by COBE). In the end, we have proposed an improved calculation formula for the damping of the Gravitational Waves through the Vacuum . Another major effect of the viscous model of the space-time is that the relative speed Earth – CMB must be reduced incrementally with the acceleration . This BRAKING phenomenon of the Earth compared with the CMB, requires the existence of an Inertial Mass independent of the presence of other bodies ! This would fundamentally contradict Mach's principle . In our opinion, the energy losses by gravitational viscosity[1]

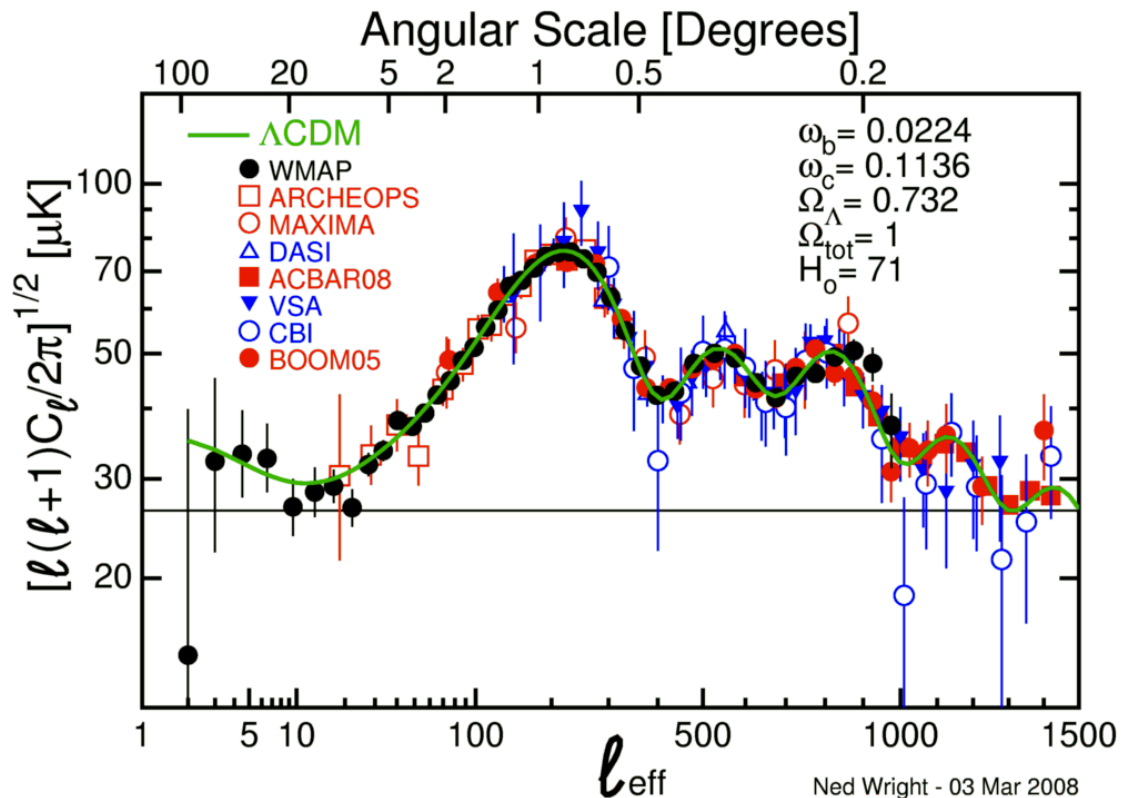represent a major cause of the irreversibility of the phenomena at a cosmological scale.

fig 1 – CMB thermal variations –anisotropies (function to solid angle) measured by COBE , WMAP , Boomerang & all.[3].
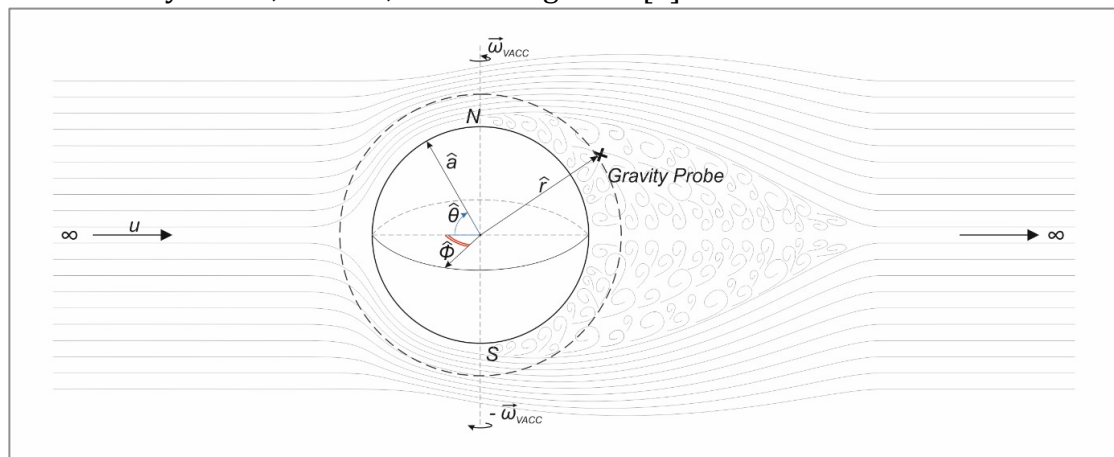

fig 2- Earth moving with u-speed trough viscous space-time ; $(\hat{r}, \hat{\theta}, \hat{\Phi}) =$ spherical coordinates ; ω_{vacc}= space-time vorticity (torsion) to the North Pole and to the South Pole ; a= Earth radius .

[1] *E Fischer*- Energy loss by gravitational viscosity –General relativity and quantum cosmology mai 2008 / pg 1-7

 [2] *A Linde* – L'inflation eternelles de l'Univers-bulles-La Recherche / oct /2006

[3] *Francis Everitt* – Gravity Probe B Final results of a space experiment to test General Relativity – abstract - Physical Review Letters 2011

 [4] *V A Belinski , I M Khalatnikov* –Influence of viscosity on the character of cosmological evolution –J.E.T.P. Soviet Union 13 march1975 pg 205-210

Thin film deposition using the pulsed laser method

Phd. Student Lazar Oana Andreea

In order to achieve multilayer thin films is used technique of pulsed laser deposition (PLD).

Pulsed laser deposition (PLD) is a physical vapor deposition (PVD) technique where a pulsed laser beam is focused inside a vacuum chamber to hit a target of the material that is to be deposited.[1]

The assembly of experimental setup it involvesusing a laser (Nd:YAG, ArFexcimer), vacuum chamber, target of the material, substrate, gas bottle, turbomolecular pump and a preliminary pump.

The process of PLD consists of utilizing a pulsed laser beam directed under an angle of 45° towards the target. The target and the substrate are situated in a vacuum chamber at a range of distance from 3 cm to 10 cm. When the pulsed laser beam strikes the target, it's said that occurs the absorbtion of photons by the target material.[2]

Therefore, we say than appear the ablation process in which a quantity of material is removed from the target in the form of plasma plume and deposited on the substrate.

When it occurs the phenomena of laser – target interaction, energy is converted to electronic excitation and then into thermal, chemical and mechanical energy.

Thus, it is resulting in evaporation, ablation and plasma plume formation. The plasma plume expands and condenses onto the substrate as thin film.[3]

The operating principle can be seen in the next figure.

[4]
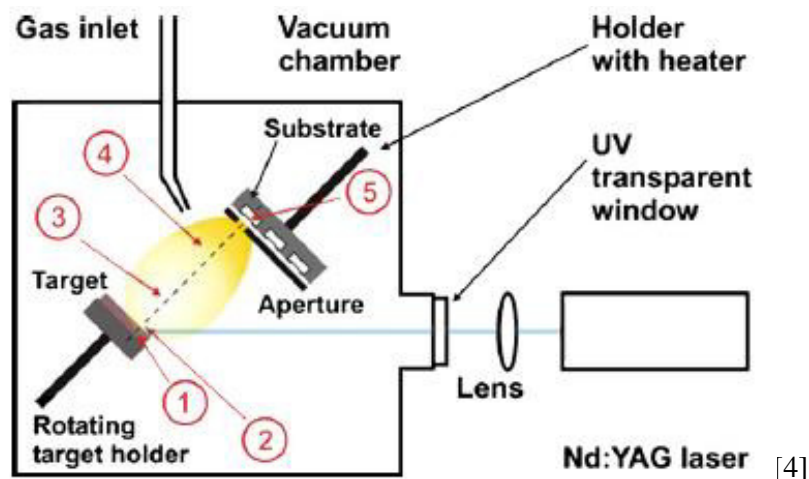
The ablation process can occurs at atmorpheric pressure (10^{-2} mbar) or in ultra – high vacuum ($10^{-7} – 10^{-12}$ mbar)in the presence of a background gas (reactive: O_2, N_2 or inert: Ar, He, Ne). The pressure control is achieved by turbomolecular and preliminary pump.

Usually, the growth modes of thin films in PLD processare: step – flow growth, layer – by – layer growth and islands growth. [1]

The growth of multilayer thin films can be influenced by the laser paramaters (the fluency and the pulse energy), the background gas pressure (the stoichiometry compounds) and the substrate parameters (temperature).

Consequently, the PLD is a frequently used method which helps to stoichiometric transfer from the target material to the substrate like a thin film.

References:

[1] Robert Eason, "Pulsed laser deposition of thin films: aplications – led growth of functional materials", John Wiley & Sons, Inc, 2007

[2]Christof W. Scheinder, Thomas Lippert , "Chapter 5: Laser Ablation and Thin Film Deposition", Paul ScherrerInstitut

[3] G. Muller, M. Konijnenberg, G. Krafft, C. Schultheiss, "Science and Technology of Thin Films", edited by F. C. Matacolta and G. Oltaviani (World Scientific, Singapore, 1995) 89

[4] J. Schou, Applied Surface Science 255 (2009) 5191 – 5198

High grade decontamination of Ni targets for sub-barrier transfer reactions

Andreea Mitu[1,2], *Marius Dumitru*[3], *Florian Dumitrache*[3], *Nicolae Marginean*[1], *Rareş Şuvailă*[1], *Cristina Niţă*[1], *Maria Dinescu*[3], *Gheorghe Căta -Danil*[2]

[1]Horia Hulubei-National Institute for Physics and Nuclear Engineering (IFIN-HH), 30 Reactorului Street, 077 125, Magurele, Romania
[2]University Politehnica of Bucharest, 313 Splaiul Independentei, Bucharest, Romania
[3]National Institute for Laser, Plasma and Radiation Physics (INFLPR), 409 Atomistilor Blvd., Magurele, Romania

e-mail: andreea.mitu@nipne.ro

Keywords:thermal treatment, sub-barrier transfer reactions

Sub-barrier neutron transfer reactions with ^{18}O or ^{13}C have a high spectroscopic potential which has been recently proven in several successful experiments with the RoSPHERE array in Bucharest. However, special care must be provided in this kind of experiments in order to avoid contamination of gamma spectra: if chemical contaminants such as Oxygen are present in the target, thereaction cross-section on these contaminants is much higher than in the case of the reaction of interest.

This work concerns the 2 neutron transfer reactionof ^{18}O beam on a ^{64}Ni target at sub-barrier energies. For this experiment were prepared thin ($\sim$1mg/ cm^2) and thick ($\sim$5mg/ cm^2) metallic layers of ^{64}Ni with high-purity (99.53% certified enrichment)and with good thickness uniformity on the defined surface.The preparation process started from the metallic powder and followed a series of steps (pressing, heating with an electron-gun and finally rolled), until the required thickness and uniformity were achieved.During the target preparation process, due to the known chemical activity of the Ni powder with the air components, atomic layers of Oxygen are incorporated and also formed on the target surface.

For the experimental energy range, the ^{18}O beam induced nuclear reactions on the^{16}O at the target surface. This is a major drawback, since gamma rays coming from the reactions on ^{16}O bring a significant contribution in the gamma energy spectrum. In order to overcome it, a thermal treatment with a hydrogen oven was applied.

The performances of the targets after the thermal treatmentshowedan important reduction of the Oxygen contamination.

The study of *p*-Si/TiO₂/*n*-Si (100) sandwiches structures deposited by KrF excimer laser ablation

Calin Moise[1*], Alin Jderu[1], Oana Brincoveanu[1,2],
Dionizie Bojin[1], Marius Enachescu[1]

[1]Center for Surface Science and Nanotechnology, Politehnica University of Bucharest, 060042, Romania
[2]University of Bucharest Faculty of Physics P.O. Box MG-11, Magurele, Ilfov, 077125 Romania
*calin.moise@cssnt-upb.ro

Abstract: Laser ablation is a versatile technique for deposition of metals, semiconductors as well as dielectrics. Our pulsed laser deposition (PLD) system is set up into an ultra-high vacuum (UHV) machine with working pressure of $8.5*10^{-11}$Torr. In this work we report the successfully deposition of sandwiches structures *p*-Si/TiO₂/*n*-Si (100) substrate. The obtained thin layers were characterized by atomic force microscopy (AFM), scanning electron microscopy (SEM) and composition was investigated by energy dispersive X-ray (EDX). Also micro-Raman spectroscopy was involved for measurement of the stress in *n*-Si (100) substrates as well as top deposited *p*-Si. The layer thicknesses were measured by ellipsometry technique. Depositions were performed at three different values for: distance between target and substrate (3, 4, 5 [cm]), temperature of substrate (400, 500, 600 [°C]), laser pulse energy (400, 500, 600 [mJ]) and laser pulse repetition rate (20, 30, 40 [Hz]). We conclude that the optimally conditions for both layersdeposition are: 5 cm, 500°C, 500mJ, and 30 Hz.

1 Introduction

The market demand for thinner field effect transistor (FET), such the 14 nm technologynow available, increased the interest of scientists for buried oxides layers. Following this trend we started to deposit successive layers TiO₂ and *p*-Sitype over a*n*-Si (100) substrate by laser ablation and to find the proper parameters for uniform surfaces.

Laser ablation is a versatile technique for deposition of: metals, semiconductors as well as dielectrics [1,2].

The TiO₂ is well known insulator with chemical stability even at high temperature, being suitable for thin buried oxide layer.

2 Experimental and results

Pulsed laser Deposition (PLD) system is a unique versatile research tool. The system offers a broad range of materials and applications. The ability to extend the vacuum capabilities to ultra-high vacuum base pressures allows the control of unwanted film impurities. Up to now, our best vacuum level is **$8.5*10^{-11}$**Torr. The laser target manipulator accommodates up to four 2" diameter wafers which are selectable through the controlling computer. Each of the individual targets can be rotated about its axis, which combined with the laser ablation scanning provides a uniform ablation of the target. Using this flexibility, a multitude of thin film structures deposition are possible.

The system consists of three chambers, load lock, growth and the RHEED gun, which serve for load/unload the targets and samples, deposition and ***in-situ*** analysis respectively.

The ablations were performed with Coherent Compex pro 205 F KrF excimer laser, havingλ = 248 nm and pulse duration of 20ns.

First step is the substrate preparation prior to deposition. The commercial (Sigma Aldrich) n-Si wafer (100) oriented surface was treated by HF 10% for 10 minutes to eliminate the native oxide from the surface, after being cleaned by acetone and dried in nitrogen flow.

The (100) surface orientation was proved by RHEED investigation (not shown here).

For studying p-Si/TiO$_2$/n-Si (100) sandwiches structures we must have the possibility to investigate both deposed surfaces, therefore after the oxide deposition the samples were taked out and a Ti foil mask was used for partial covering the surface before the deposition of p-Si layer [3].

Nanoscale investigations were carried out by AFM (Solver Next) [4,5] and reveal that optimal value of distance, temperature, laser energy, repetition rate are: 4cm, 500 , 500 mJ and 30 Hz respectively forboth deposed layers. In Figure 1 are the AFM images for TiO$_2$ deposited surface. As can be observed the quality of surface is very good (Ra and RMS below 0.6 nm).
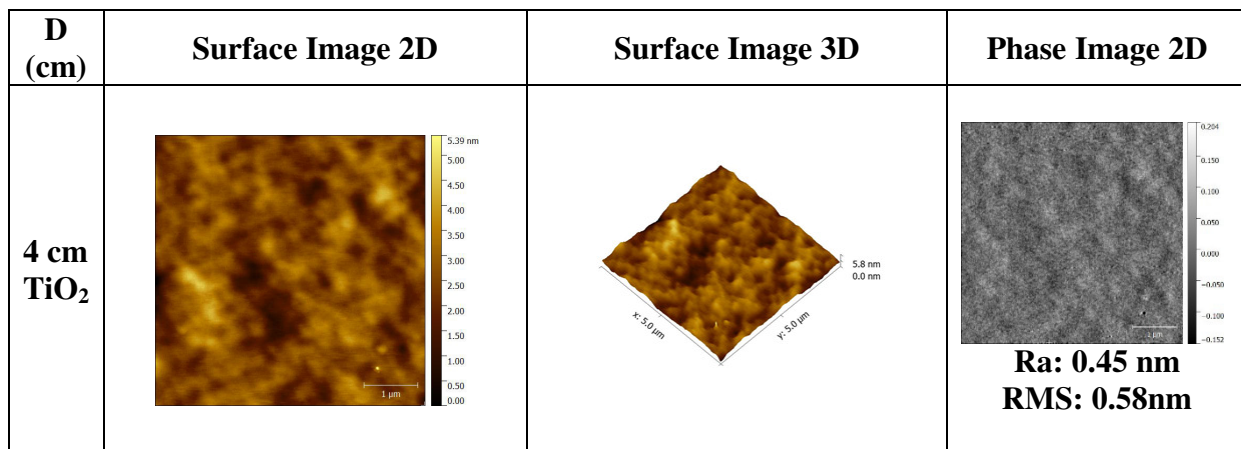
D (cm)	Surface Image 2D	Surface Image 3D	Phase Image 2D
4 cm TiO$_2$			Ra: 0.45 nm RMS: 0.58nm

Figure 1 – AFM images of TiO$_2$ surface

3 Further directions for research

Comparison with sputter deposition technique, measurement of electrical properties of the *p-n* structure modulated by buried TiO$_2$.

4 References:

1) Editor: Phipps Clude "Laser Ablation and its Applications" Springer Series in Optical Science 2007.

2) Stafe Mihai, Marcu Aurelian, Puscas Nicolae "Pulsed Laser Ablation of Solids" Springer Series in Surface Science 2014.

3) Calin Moise, Oana Brincoveanu, Adrian Katona, Dorel Dorobantu, Dionizie Bojin, Marius Enachescu"The study of p-Si/Al2O3/n-Si (100) sandwiches structures deposited by KrF excimer laser ablation" Proceeding of the 40th-ARA Montreal Canada 2016.

4) A. Moldovan, P.M. Bota, D. Dorobantu, I. Boerasu, D. Bojin, D. Buzatu, M. Enachescu "Wetting properties of glycerol on silicon, native SiO$_2$, and bulk SiO$_2$ by scanning polarization force microscopy" Journal of Adhesion Science and Technology, 28, 13, 1277-1287, (2014).

5) A. Moldovan, P.M. Bota, T.D. Poteca, I. Boerasu, D. Bojin, D. Buzatu, M. Enachescu "Scanning polarization force microscopy investigation of contact angle and disjoining pressure of glycerol and sulfuric acid on highly oriented pyrolytic graphite and aluminum" The European Physical Journal Applied Physics, 64, 31302-31308, (2013).

New digital acquisition system for a large multichannel spectroscopy array
Student: Stan Lucian

As time passes, more and more nuclei are being investigated, their properties being measured and determined. This creates an incentive for experimenters to develop new detector arrays with more channels and better characteristics. In turn, these modern nuclear experiments necessitate sophisticated multi-channel acquisition systems which can handle and process the large number of signals.

The Nuclear Physics Department of the Romanian National Institute of Nuclear Physics and Engineering in Magurele operates, among others, a 9MV Tandem accelerator. It delivers light nuclei to, among others, the RoSphere detector array, which can receive, in its 25 positions, fast LaBr3 scintillator detectors, HPGe detectors with very good energy resolution and, more recently, neutron detectors. Furthermore, RoSphere has been augmented by the addition of two mobile neutron "walls", with 12 detectors each.

Besides the addition of neutron detectors, there are plans in the department to expand RoSphere's capacities byadding more ancillary detectors to the set-up, like segmented silicon detectors. However, these plans were hampered by the acquisition system.

The old RoSphere acquisition system. It's size and impressive number of modules are readily observable. It only recorded signals from 50 channels – Source: Photo taken by the author

While appreciated as adequate in its role up to that point, it raised significant difficulties if anyexpansion was to be carried out.

Thus, it was decided to implement a new system, using new state-of-the-artsignal processing modules, which would not only allow for the expansion of theRoSphere array, but also bring up many new functionalities. For this system, acontrol program was developed, based on the open-source Gecko suite written by Bastian Loher.

The new system was ready and commissioned in September 2016. It proved capable of handling the signals from all the 25 detectors of the RoSphere array. Furthermore, new signals have been added. The time and energy from the anti-Compton shields are now recorded, allowing us to employ a multiplicity filter. The energy of the HPGe detectors is registered twice, first with a larger gain,

which allows good energy resolution, and secondly with a smaller gain, which allows us to observe gamma energies of up to 7 MeV.

A simulation of the RoSphere detector array, as it currently stands, with 10 HPGe detectors, 11
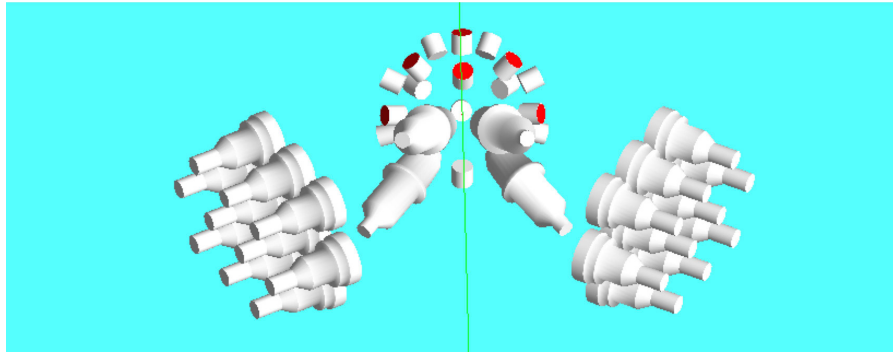
LaBr3 detectors and 26 neutron detectors – Source: N. Marginean et al., Spectroscopy and lifetime measurements of low-lying T= 0, 1 states in 62Ga, Proposal for the TANDEM accelerator for the period March 2016 - December 2016

Recently, at the end of March 2017, neutron detectors were added to the RoSphere array, and the acquisition system had to take in 76 more signals, which it has with ease.

Images
[1]The old RoSphere acquisition system. It's size and impressive number of modules are readily observable. It only recorded signals from 50 channels – Source: Photo taken by the author
[2]A simulation of the RoSphere detector array, as it currently stands, with 10 HPGe detectors, 11 LaBr3 detectors and 26 neutron detectors – Source: N. Marginean et al., Spectroscopy and lifetime measurements of low-lying T= 0, 1 states in 62Ga, Proposal for the TANDEM accelerator for the periodMarch 2016 - December 2016

Sources
[1] http://www.nipne.ro/research/departments/dfn.php
[2] D. Bucurescu et al / Nuclear Instruments and Methods in Physics Research A 00 (2016)
[3] C. R. NITA et al., Fast-timing lifetime measurements of excited states in 67Cu, PHYSICAL REVIEW C 89, 064314 (2014)
[4] N. Marginean et al., Measurements of sub-nanosecond nuclear lifetimes with an array of HPGe and LaBr3 detectors, Eur. Phys. J. A 46, 329336 (2010)
[5] http://www.mesytec.com/products/datasheets/MSCF16-LN.pdf
[6] http://www.mesytec.com/products/datasheets/MADC-32.pdf
[7] http://www.mesytec.com/products/datasheets/MTDC-32.pdf
[8] http://www.struck.de/pcivme.htm[14] Ortec: Electronic Standards and Definitions,www.ortec-online.com/download/electronics-standards-definitions.pdf
[9] http://www.wiener-d.com/sc/powered-crates/vme/
[10] http://www.osti.gov/scitech/biblio/7120327
[11] The defunct ESONE website https://esone.web.cern.ch/ESONE/
[12] http://pinouts.ru/Slots/vmebus_pinout.shtml
[13] Gamma-ray spectroscopy with a LaBr3 :(Ce) scintillation detector at ultra high count rates, Master thesis, Bastian Lher, November 2010,http://www.ldot.de/mediawiki/images/Master_thesis.pdf
[14] http://www.gnu.org/licenses/lgpl-3.0.en.html
[15] N. Marginean et al., Spectroscopy and lifetime measurements of low-lying T= 0, 1 states in 62Ga, Proposal for the TANDEM accelerator for the periodMarch 2016 - December 2016
[16] http://www.sparrowcorp.com/downloads/kmax-9-0
[17] A.Turturica, Private Communication

Assessment of a Hybrid Acquisition System for Positron Annihilation-based Spectroscopy

Sebastian Toma [1, 2]
[1] PhD student, Faculty of Applied Sciences, University
POLITEHNICA of Bucharest, Romania
[2] Department of Nuclear Physics, "Horia Hulubei" National Institute
for Physics and Nuclear Engineering, Măgurele, Romania

A hybrid (digital and analogic) data acquisition system for Positron Annihilation Spectroscopy is described. Results of comparative testing measurements using pairs of the same HPGe detectors using both purely digital and analogic setups reported

1. Introduction

 Positron Annihilation Spectroscopy (PAS) is a class of non-destructive techniques used for materials testing, based on the implantation of positrons from radioactive sources into the samples and followed by measurements of the annihilation characteristics. These characteristics are strongly influenced by trapping of positrons inn vacancy-type defects and thus make the PAS excellent tools for defects detection (dislocations, vacancies, clusters) in the material microstructure. The LaMAR laboratory at Politehnica University uses two methods of PAS technique: Positron Annihilation Lifetime Spectroscopy (PALS) and Coincidence Doppler Broadening Spectroscopy (CDBS) currently implemented in a classical manner (i.e. analogic measurement chain).

2. Experimental Setups

The two methods already available at LaMAR are:
1. Positron annihilation lifetime spectroscopy (PALS). Details on the turn-key system can be seen in [1] and [2].
2. Coincidence Doppler Broadening Spectroscopy (CDBS): This method exploits the lineshape of the 511 keV annihilation gamma-rays. [3].
 Given the advent of digitizers [4], data acquisition systems can be simplified while at the same time offer more flexibility in treating the recorded data. In the past decade, a series of digital spectrometers for PAS have been developed [3][5][6], making use of the *waveform*-mode of operation, with offline treatment of the *raw data*.
 The XIA DGF4C rev.F digitizers used in the present work are designed for operating with HPGe detectors by internal FPGA *filtering and shaping* of the raw preamplifier signals, while also providing an *integration* mode of operation.
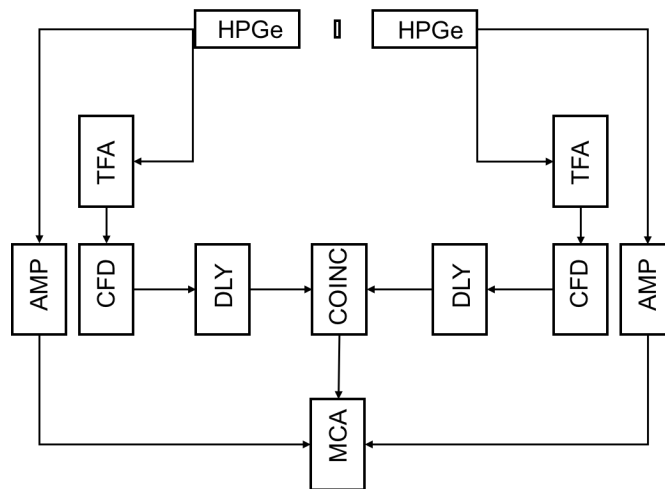
Fig. 1 – Block-diagram of the analogic CDBS system

In effect, this eliminates the need for preprocessing HPGe signals. The drawback is the low sampling rate, making the typical timing resolutions required for lifetime measurements unachievable without extra modules. Thus, a hybrid system has been set up (Figure 2).
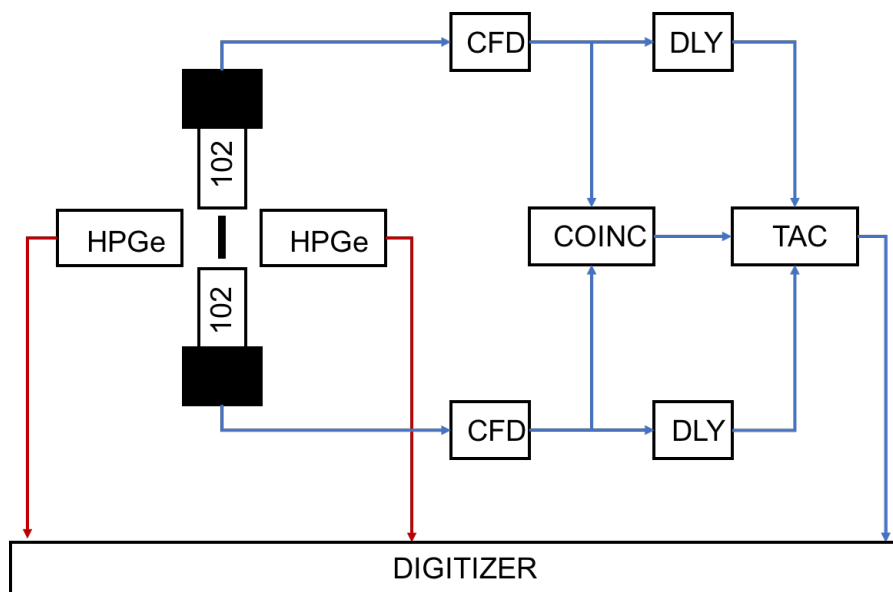

Figure 2 – Block-diagram of the Hybrid system. Both PALS and CDBS can be run simultaneously. [red] HPGe preamp signals fed directly to the digitizer. [blue] analogic pre-processing for PALS

3. References

[1] Paulus, T.J. – China Nuclear Society Seminar, Beijing, China, 1995
[2] PLS-System – Positron Lifetime Picosecond Timing System Datasheet, http://www.ortec-online.com
[3] Cizek, A – NIM A 623 (2010) 982-994
[4] Warburton, W.K. – Appl. Radiat. Isot. 2000 Oct; 53(4-5):913-20
[5] Nissila, J. – NIM A 538 (2005) 778-789
[6] Becvar, F. – NIM A 539 (2005) 372-385